Preliminary results from an electromagnetic groundwater flow measurement system

Michael Hayes, Ben Mitchell, Blair Bonnett, and Bill Heffernan
Department of Electrical and Computer Engineering
University of Canterbury
Christchurch, New Zealand

***Abstract*—Groundwater makes up the majority of the world's fresh water. Modelling these flows requires verification against measured data. Currently this data is obtained from monitoring wells, a complex and expensive task. A proposed electromagnetic measurement system would simplify the collection of ground truth values and allowed improved model tuning. This technique requires measurement of sub-microvolt scale signals in the presence of large interference. A test system has been developed to validate the technique, and this paper presents some preliminary results from initial testing. Experiments show that significant harmonic distortion is present and that the signal levels fluctuate. Both these effects appear to be due to the electrode-electrolyte interfaces.**

I. Introduction

Given underground flows make up the majority of the world's freshwater, modelling these flows is important to guide land use practices [1]–[3]. Topographical features such as lakes, rivers, and vegetation, soil composition, and geological factors all influence the flow [4]. Although complex, currently models are only validated by a small number of measurements taken using underground wells. The cost and complexity of drilling further wells is problematic.

As part of Spearhead 2 of the Science for Technological Innovation (SfTI) National Science Challenge (NSC), a new technique for measurement groundwater is being investigated. This operates by generating a magnetic field and measuring the induced electric field caused by water ions moving through this magnetic field [5]. By eliminating the need for monitored wells, this would simplify groundwater measurements and allow improved model tuning. Initial simulations have shown that the induced voltages will be miniscule: for a typical water flow of 10 mm/hr in a 10 mT magnetic field, electrodes spaced 1 m apart will record a potential difference on the order of 10 nV [5]. The main interfering signal will be the direct induction from the magnetic field into the measurement loop formed by the electrodes. This can be several orders of magnitude larger than the desired signal and is at the same frequency, but 90 degrees out of phase. Careful measurement and synchronous processing will allow this to be separated from the flow signal.

A prototype system is being used to prove the concept in laboratory testing. This paper presents some preliminary results from this testing. The system is introduced in Section II and models for the source impedance and signals are presented in Sections III and IV, respectively. The signal processing to extract the desired signal is explain in Section V, followed by some experimental results in Section VI. Finally, a discussion and conclusions are presented in Sections VII and VIII.

II. Test setup

A rectangular tank, shown in Fig. 1, has been constructed to perform initial testing of the system. The tank is constructed from 23 mm thick acrylic sheets. It is 2.1 m long and 1.2 m wide with a height of 600 mm. It is divided into three chambers lengthwise with the two end chambers being 225 mm long. A grid of holes is drilled into the acrylic separating the chambers so that water can flow the length of the tank. In operation, water is drained from one of the end chambers and pumped into the other creating a lengthwise water flow. This flow can be created in either direction. Each end chamber contains a pair of baffles which are used to set the head height of the water and thus the flow speed. The baffles also remove the turbulence caused by pumping water into the chambers.

Once the preliminary testing has been completed, sand will be placed into the main chamber to simulate the underground environment. The sand alone will weigh on the order of 2 tons. To support this weight, the tank is reinforced by a number of external fibreglass beams.

The source of the magnetic field is a coil placed under the centre of the tank. This is connected in series to a capacitor bank which tunes the system to the operational (resonant) frequency $f_0 = 16.8$ Hz. This is driven by an Ametek MX45 power source at currents up to 300 A. Initial testing shows the magnetic field produced in the vertical or z direction, B_z, is approximately 3 mT at an excitation current of 50 A. This will scale linearly with the current. Note that having the coil under the tank is functionally equivalent to having the coil on top of the Earth's surface in the final system.

The induced electric field is measured between a pair of electrodes. As shown in Fig. 2, these electrodes are constructed from a ring of copper 12 mm wide. A probe consists of five electrodes mounted on a 25 mm PVC pipe at intervals of 100 mm. The bottom electrode is 65 mm above the bottom of the probe. A screened cable connects the electrodes to the receiver electronics. The probes are placed vertically in the tank, forming a line perpendicular to the direction of water flow as shown in Fig. 1.

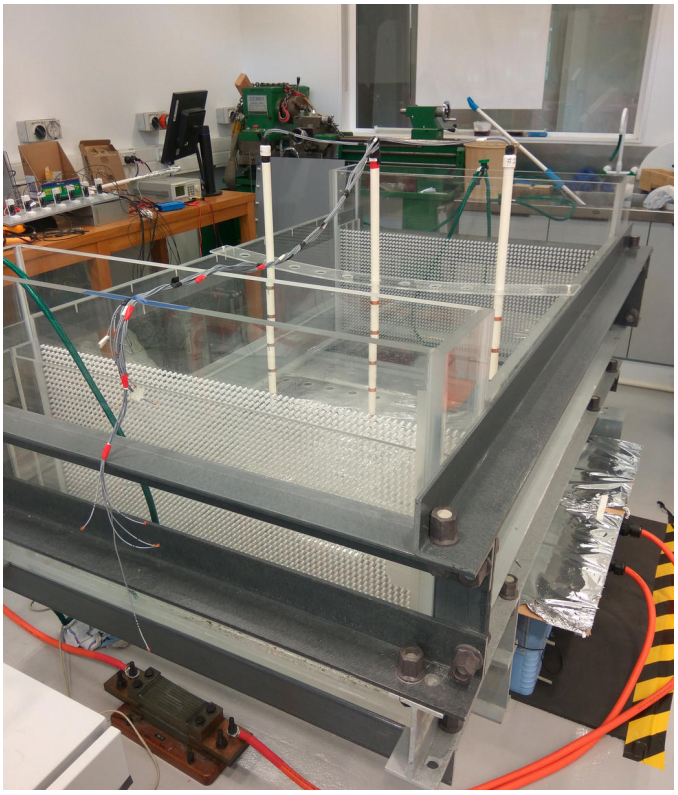

Fig. 1. The test setup. The tank is made from acrylic and is supported by fibreglass beams. The coil sits on a pallet (the blue object just visible at the bottom-right) under the tank and is connected to a capacitor bank and power source, neither of which are shown here. Three measurement probes, each with five copper electrodes, are placed across the centre of the tank.

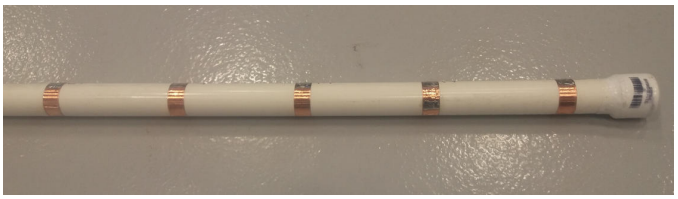

Fig. 2. A probe, constructed from a PVC pipe with five copper electrodes spaced along its length.

III. Source Model

Many models have been proposed to model the impedance of two electrodes in an electrolyte. A common model is the Randles model shown in Fig. 3. This uses a type of constant phase element known as Warburg element with an impedance $Z_W(\omega) = A\,(\mathrm{j}\omega)^{-0.5}$. Another model commonly used to represent the electrode-tissue interface (ETI) for medical applications [6] is shown in Fig. 4. This uses a generic constant phase element with an impedance $Z_{\mathrm{CPE}}(\omega) = A\,(\mathrm{j}\omega)^{-n}$. Note, when $n = 0$ this describes the impedance of a resistor and when $n = 1$ this describes the impedance of a capacitor.

The impedance of the electrodes in the tank was measured with a Keysight E4990A Impedance Analyzer for two different probe separations in water and with a range of water depths above the electrodes. The impedance was measured over a frequency range 20 Hz–10 kHz. No bias was applied.

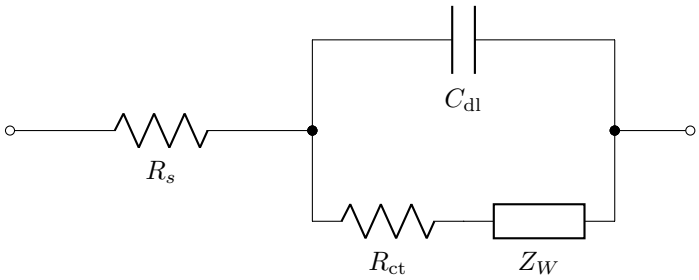

Fig. 3. Randles model for the impedance between the two electrodes. Z_W is the impedance of a Warburg element, R_{ct} is charge-transfer resistance, C_{dl} is the combined interfacial capacitance of the electrodes due to the Helmholtz double layer and diffuse layer, and R_s is the spreading resistance through the water (and the negligible cable resistance). This model neglects the capacitance between the electrodes.

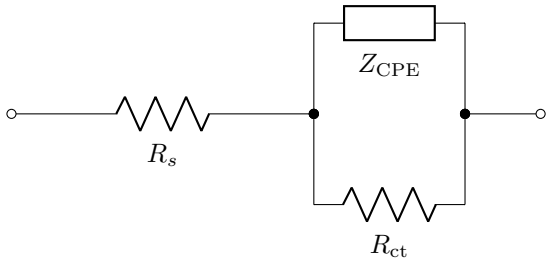

Fig. 4. Model commonly used for the electrode-tissue interface (ETI) for medical applications. Z_{CPE} denotes a general constant phase element with impedance $Z_{\mathrm{CPE}}(\omega) = A(\mathrm{j}\omega)^{-n}$.

Once the source impedance was measured it was fitted to the models shown in Fig. 3 and Fig. 4 using a non-linear least squares optimisation to find the minimum variation between the absolute value of the measured and modelled impedances. The results are shown in Fig. 5 and Fig. 6. Both models provide a good fit above 100 Hz but below 100 Hz the generalised constant phase element model is more accurate. The impedance is dominated by the spreading resistance through the water between the electrodes. This depends upon the electrode surface area, water conductivity, and water depth. The estimated value for R_{ct} for the general constant phase element model is so large that it has negligible effect and can be removed from the model.

IV. Signal Model

The measured voltage at the input of the preamplifier can be separated into four components.

$$v_i(t) = v_{if}(t) + v_{im}(t) + v_{ie}(t) + v_{in}(t), \qquad (1)$$

where $v_{if}(t)$ is the desired voltage induced by the water flow through the magnetic field, $v_{im}(t)$ is the interference due to coupling of a changing magnetic flux through the measurement loop (transformer signal), $v_{ie}(t)$ is the interference due to capacitive coupling of the electric field across the coil, and $v_{in}(t)$ is the input referred noise. The noise is primarily generated by the source resistance and the preamplifier.

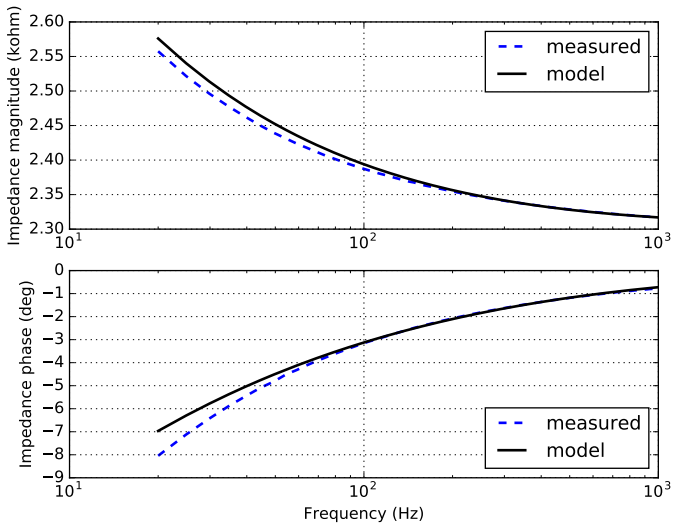

Fig. 5. Measured source impedance with fitted Randles circuit (water depth 100 mm). The best fit parameters are $R_s = 2.3\,\mathrm{k}\Omega$, $C_{\mathrm{dl}} = 3.0\,\mu\mathrm{F}$, $Z_w = 5.1 \times 10^3 (\mathrm{j}\omega)^{-0.5}$, $R_{\mathrm{ct}} = 4.1 \times 10^{-6}\,\Omega$.

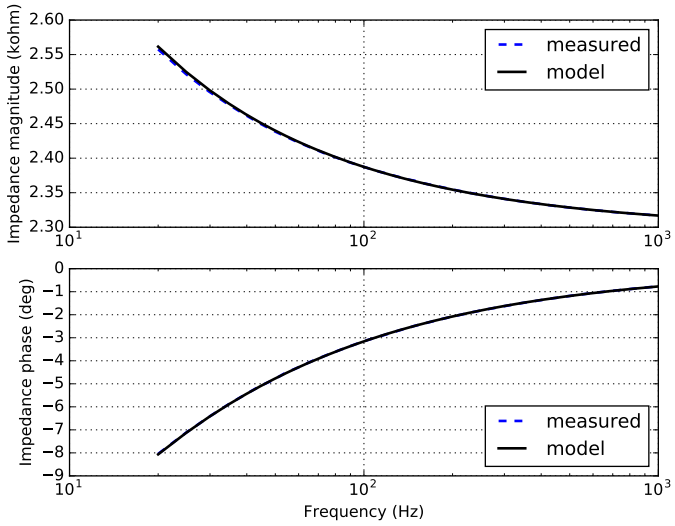

Fig. 6. Measured source impedance with fitted generalised constant phase element circuit (water depth 100 mm). The best fit parameters are $R_s = 2.2\,\mathrm{k}\Omega$, $Z_{\mathrm{CPE}} = 9.0 \times 10^3 \times (\mathrm{j}\omega)^{-0.63}$, $R_{\mathrm{ct}} = 200 \times 10^9\,\Omega$.

For AC excitation of the coil, it is useful to consider the measured signal in the frequency domain,

$$V_i(\omega) = V_{if}(\omega) + V_{im}(\omega) + V_{ie}(\omega) + V_{in}(\omega). \tag{2}$$

With reference to Fig. 7, V_{if} is generated by V_f, V_{im} is generated by V_m, and V_{ie} is generated by V_e. The noise voltage sources are not shown for clarity.

The signal of interest, $V_{if}(\omega)$, is proportional to the voltage induced by the water flow, $V_f(\omega)$. This can be determined from the flowmeter equation [5] and is described by

$$V_f(\omega) = KSB_z(\omega)v_w, \tag{3}$$

where K is a constant, S is the probe separation, B_z is the z-component of the magnetic field, and v_w is the water speed (in the y-direction). This expression assumes the water flow is orthogonal to the magnetic field. The magnetic field is proportional to, and in phase with, the current through the coil, $I(\omega)$,

$$B_z(\omega) = k_b I(\omega), \tag{4}$$

where k_b is a constant of proportionality that varies spatially. There will be a slight spatially variant phase shift due to retardation of the fields but this can be neglected at low excitation frequencies. After combining (4) with (3), the flow signal has the form,

$$V_f(\omega) = k_f v_w I, \tag{5}$$

where k_f is a scale factor.

The measured flow voltage depends upon the source impedance. From Fig. 7,

$$V_{if}(\omega) = H_f(\omega)V_f(\omega), \tag{6}$$

where the transfer function, $H_f(\omega)$ is given by

$$H_f(\omega) = \frac{Z_i(\omega)}{Z_i(\omega) + Z_E(\omega) + R_s \parallel Z_e(\omega)} \frac{R_s \parallel Z_e(\omega)}{R_s}. \tag{7}$$

where Z_i is the preamplifier input impedance, R_s is the spreading resistance through the water between the electrodes, and Z_E is the impedance of the electrode-electrolyte interfaces.

The magnetic interference signal (transformer signal), $V_m(\omega)$, results from the changing magnetic flux from the coil inducing a voltage in the measurement loop as described by Faraday's law. Since the magnetic field is proportional to the coil current, $I(\omega)$,

$$V_m(\omega) = \mathrm{j}\omega k_m I(\omega), \tag{8}$$

$$= \alpha_m(\omega) \exp(\mathrm{j}\phi_m)\, I(\omega), \tag{9}$$

where k_m is a constant (the mutual inductance) that is dependent on the fraction of the measurement loop area that intercepts the changing magnetic flux from the coil. In theory, the transformer signal is zero if the measurement loop is aligned with the magnetic field but this difficult to achieve in practice. Since the induced voltage depends on the rate of change of the magnetic flux, it is desirable to use a low excitation frequency.

With reference to Fig. 7, the measured transformer signal is

$$V_{im}(\omega) = H_m(\omega)V_m(\omega), \tag{10}$$

where $H_m(\omega) = H_f(\omega)$, as described by (7).

The principle source of electrical interference is the electric field across the coil. This can be modelled as

$$V_e(\omega) = \alpha_e(\omega) \exp(\mathrm{j}\phi_e(\omega))\, I(\omega), \tag{11}$$

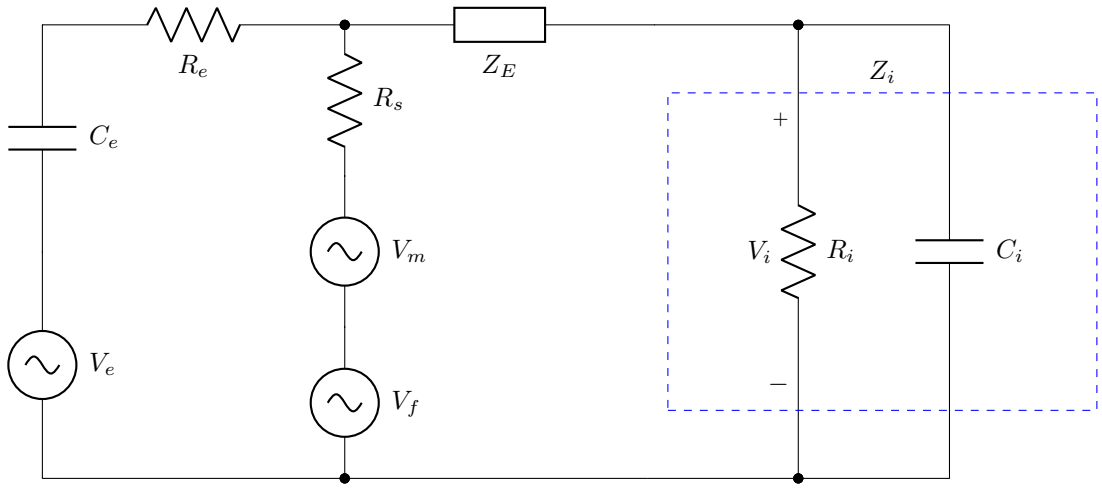

Fig. 7. Simplified electrical circuit model: V_f models the voltage produced by the water flow, V_e is the capacitively coupled electric field interference, V_m is the inductively coupled magnetic field interference (transformer signal), R_s is the spreading resistance through the water between the electrodes, Z_E is the impedance of the electrode-electrolyte interfaces, modelled by a constant phase element, C_e is the electric interference coupling capacitance, R_e is the electric interference coupling resistance in the water, R_i is the preamplifier input resistance, and C_i is the preamplifier input capacitance. This model neglects the capacitance between the electrodes and the inductance of the measurement loop. It also omits the noise sources for clarity.

where

$$\phi_e(\omega) = \tan^{-1}\frac{\omega L}{R}, \tag{12}$$

and

$$\alpha_e(\omega) = k_e\sqrt{(\omega L)^2 + R^2}. \tag{13}$$

In these equations, k_e is a constant, R denotes the coil resistance, and L denotes the coil inductance. It is worth noting that the electrical interference, $V_e(\omega)$, is not in perfect phase-quadrature with the coil current, $I(\omega)$, due to the resistance of the coil.

The transfer function for the electrical interference is

$$H_e(\omega) = \frac{V_{ie}(\omega)}{V_e(\omega)}, \tag{14}$$

$$= \frac{Z_i(\omega)}{Z_i(\omega) + Z_E(\omega) + R_s \parallel Z_e(\omega)} \frac{R_s \parallel Z_e(\omega)}{Z_e(\omega)}, \tag{15}$$

where

$$Z_e(\omega) = R_e - \mathrm{j}\frac{1}{\omega C_e}, \tag{16}$$

is the Thévenin impedance for the electrical interference.

Provided the input impedance is many orders of magnitude greater than the source impedance, the transfer functions can be approximated by

$$H_e(\omega) \approx \frac{R_s}{R_s + Z_e(\omega)}, \tag{17}$$

$$H_m(\omega) = H_f(\omega) \approx \frac{Z_e(\omega)}{R_s + Z_e(\omega)}. \tag{18}$$

At low frequencies, $|Z_e(\omega)| \gg R_s$ and so,

$$H_e(\omega) \approx \frac{R_s}{Z_e(\omega)} \approx \mathrm{j}\omega R_s C_e, \tag{19}$$

$$H_m(\omega) \approx 1. \tag{20}$$

Using these approximate transfer functions and the fact that $\phi_m(\omega) \approx \pi/2$, the phase shift between the electrical and magnetic components of the interference is $\phi_e(\omega)$.

To be able to separate the flow signal from the quadrature transformer signal it is necessary to have a reference signal. This is achieved using a single-turn search coil placed above the coil [7]. This arrangement maximises the signal to noise ratio of the reference signal and reduces the capacitance of the search coil. A low capacitance increases the resonant frequency of the search coil and thus reduces the phase shift [8]. Since the voltage from the search coil depends on the rate of change of the magnetic field, and the latter is proportional to the coil current, the reference signal can be described by

$$V_r(\omega) = \mathrm{j}\omega k_r I(\omega), \tag{21}$$

$$= \alpha_r(\omega)\exp\left(\mathrm{j}\phi_r(\omega)\right) I(\omega), \tag{22}$$

where $\phi_r(\omega) \approx \pi/2$.

V. Signal Processing

The signal processing goal is to estimate the water speed, v_w, from the measured signal, $v_i(t)$, using the reference signal, $v_r(t)$. The first step is to bandpass filter the reference and measured signals and convert them to their complex-envelope representations. After this, the reference signal has the form

$$\tilde{r}(t) = k_r I \exp\left(\mathrm{j}\phi_r\right) + \tilde{n}_r(t). \tag{23}$$

and the measured signal has the form

$$\tilde{v}_i(t) = k_f v_w I + \mathrm{j}k_m I + \mathrm{j}k_e \exp\left(\mathrm{j}\phi_e\right) I + \tilde{n}(t), \tag{24}$$

where I denotes the amplitude of the coil current. Note, since ϕ_e is close to $\pi/2$ radians, the second term due to the electrical interference is mostly in phase with the flow signal represented by the first term.

The second step is to calculate the Hermitian product of the measured signal complex envelope with the phase-corrected reference signal. To compensate for fluctuations in coil current, the Hermitian product is normalised by the magnitude of the reference signal,

$$\tilde{x}(t) = \frac{\tilde{v}_i(t)\tilde{r}^*(t)\exp\left(\mathrm{j}\phi_r\right)}{|\tilde{r}(t)|}. \tag{25}$$

Here $*$ denotes the complex conjugate operator.

VI. Results

An experiment was performed where the RMS coil current was varied with a profile of 150 A, 100 A, 50 A, 100 A, 150 A. Each current step lasted for 600 s. The voltage between the electrodes was recorded for the first half of each current step. For calibration purposes, the voltage between a similar pair of electrodes was recorded for the second half of each current step. These electrodes were out of the water. For this experiment, the transformer signal was minimised by slightly displacing the electrodes. The water was stationary to assess the levels of the interfering signals.

The results of the experiment are shown in Fig. 8. Note, the glitches are an artefact of switching between electrodes. The real component of the signal is due to electrical interference and the imaginary component is primarily due to the residual transformer signal plus a component of the electrical interference. A surprising result is that the electrical interference is not proportional to the coil current as predicted by (11). In addition, there is more variation in the signal amplitude than would be expected from the signal to noise ratio.

It was observed from the data that there was considerable harmonic distortion. This was quantified by varying the coil excitation current and measuring the fundamental component and its third harmonic. This relationship is plotted in Fig. 9. The copper electrodes were replaced by stainless steel (type 304) electrodes (albeit slightly larger) and the experiment was repeated. A similar non-linear relationship was observed as shown in Fig. 10.

VII. Discussion

Flowmeters suffer interference from unwanted magnetic and electric field coupling. The transformer signal due to magnetic coupling is in phase-quadrature to the flow signal and can be removed with phase-coherent processing. However, the electric field is mostly in phase with the desired flow signal and the in-phase component of this can swamp the desired weaker flow signal. Hence, it is necessary to reduce the electric field coupling. It is unlikely that it can be substantially reduced by careful calibration and modelling of the signals. Thus it will be necessary to either more thoroughly screen the coil and feed cables with a thin metallic shield and/or reduce the coil excitation frequency.

A metallic screen will slightly attenuate the magnetic field and thus reduce the flow signal. In addition, eddy currents flowing in the shield will introduce a phase shift of the magnetic field. If this is not compensated in processing, then

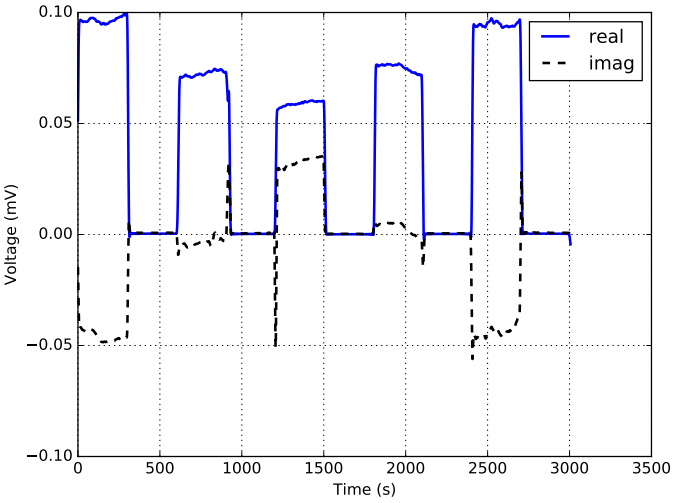

Fig. 8. No flow, processed measured signal. The real component is in phase with the magnetic field and the imaginary component is in phase-quadrature with the magnetic field.

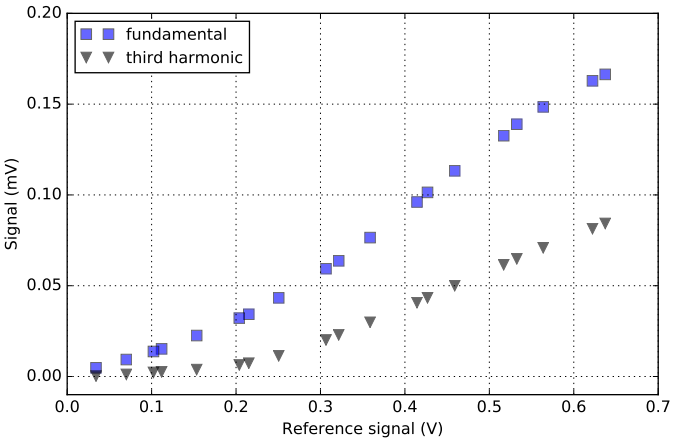

Fig. 9. The relationship of the fundamental and third harmonic as a function of coil excitation current for copper electrodes. A reference voltage of 0.5 V corresponds to a coil current of 100 A RMS.

a component of the transformer signal will be mistaken for the flow signal.

If the coil excitation frequency is reduced to DC then there is no coupling of the electric and magnetic fields. Usually a switched DC signal is employed to remove offsets, say due to galvanic effects. The disadvantage of operating at low frequencies is that $1/f$ noise is larger and thus longer integration times are required for a desired signal to noise ratio.

Another disadvantage of operating at DC is that there can be a residual difference between the two electrode's half-cell potentials which is not always stable [9]. This residual potential difference fluctuates randomly even when using identical electrodes in the same electrolyte. In addition, the

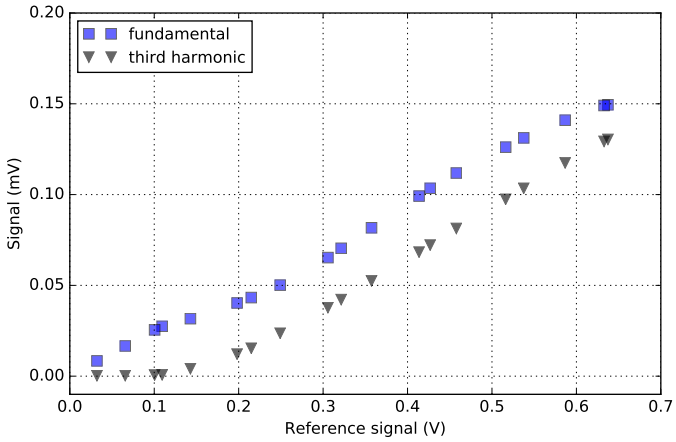

Fig. 10. The relationship of the fundamental and third harmonic as a function of coil excitation current for type 304 stainless steel electrodes. A reference voltage of 0.5 V corresponds to a coil current of 100 A RMS.

double layer at the electrode/electrolyte interface is a region of charge gradient and so disturbance of it, say due to turbulent flow, gives rise to voltage fluctuations [10].

Electromagnetic flowmeters are known to suffer from zero offsets and zero drift [11], [12]. There are many sources of drift. One cause is due to changes in the phase of the electric interference, ϕ_e, with the temperature of the coil. A more prominent effect appears to be due to variations at the electrode-electrolyte interface. The zero offset is primarily due to the transformer signal not being exactly in phase-quadrature with the flow signal [13].

There are additional small phase shifts that need consideration when low water speeds are to be measured. One occurs due to displacement currents in the water. These are ninety degrees out of phase compared to the much larger conduction currents [11]. In addition, there will be a tiny phase shift due to retardation effects although these can be compensated by calibration.

Power dissipated in the coil will result in its temperature rising and thus increase the coil resistance. With the coil being excited by a constant current, the increased resistance leads to an increase in power dissipation. Depending on the magnitude of the current and the cooling capacity available, this process will either reach an equilibrium or lead to thermal runaway. The increase in coil resistance will also lead to an increase in the voltage across the coil and thus the magnitude of the interfering electric field. However, at the operating frequency this is dominated by the reactance of the inductive component of the coil (1.1 Ω compared to the 95 mΩ coil resistance). Modelling the thermal properties of the coil suggests an increase in the coil voltage of 0.03 % for an hour-long experiment with an RMS excitation current of 50 A.

The non-linear variation of the measured electrical interference with coil current and the harmonic distortion is likely to be due to a non-linearity at the electrode-electrolyte interfaces. It has been observed in the literature that the electrode-tissue interface (ETI) for medical applications is non-linear [6]. The I-V characteristic of this interface is non-linear and thus it is postulated that the electrical circuit model in Fig. 7 could be improved by augmenting it with a pair of back-to-back diodes in series with Z_E.

VIII. Conclusion

Further work is required to quantify the I-V characteristics of the electrode-electrolyte interfaces and reassess the source model at lower voltages. However, for small flow voltages the distortion produced by this non-linearity should be insignificant. More pressingly, a reduction in the electric field interference is required. Ultimately, for the system to work for small flow rates, the variation in signal amplitude with time needs to be resolved.

Acknowledgements

This work is funded as part of the Science for Technological Innovation (SfTI) National Science Challenge (NSC) by the Ministry of Business, Innovation and Employment (MBIE). The authors would also like to thank the technical staff of the Department of Electrical and Computer Engineering at the University of Canterbury for their invaluable assistance with this project.

References

[1] P. White, M. Rosen *et al.*, "Groundwater resources in New Zealand." *Groundwaters of New Zealand*, pp. 45–75, 2001.

[2] A. P. Lovett and S. G. Cameron, "Development of a national groundwater atlas for New Zealand," Tech. Rep., 2014.

[3] M. Moreau and M. Bekele, "Groundwater component of the water physical stock account (WPSA)," Tech. Rep., 2015.

[4] R. A. Freeze and J. A. Cherry, "Groundwater," Tech. Rep., 1979.

[5] M. P. Hayes and I. Platt, "A preliminary investigation of an electromagnetic groundwater flow measuring device," in *ENZCon 2016*, Wellington, New Zealand, Nov. 2016, pp. 1–6.

[6] A. Richardot and E. McAdams, "Harmonic analysis of low-frequency bioelectrode behavior," *IEEE transactions on medical imaging*, vol. 21, no. 6, pp. 604–612, 2002.

[7] B. G. Mitchell, B. C. Bonnett, and M. P. Hayes, "Measurement of nanovolt-scale signals for electromagnetic groundwater flow determination," in *ENZCON'17, Electronics Conf. New Zealand*, Christchurch, New Zealand, Dec. 2017, pp. 1–6.

[8] S. Tumanski, "Induction coil sensors-A review," *Measurement Science and Technology*, vol. 18, no. 3, p. R31, 2007.

[9] A. I. Maalouf, "A validated model for the electromagnetic flowmeter's measuring cell: Case of having an electrolytic conductor flowing through," *IEEE Sensors Journal*, vol. 6, no. 3, pp. 623–630, 2006.

[10] C. Rosales, M. Sanderson, and J. Hemp, "Problems in the theory and design of electromagnetic flowmeters for dielectric liquids. Part 2a: Theory of noise generation by turbulence modulation of the diffuse ionic charge layer near the pipe wall," *Flow Measurement and Instrumentation*, vol. 13, no. 4, pp. 155–163, 2002.

[11] J. Hemp and I. Youngs, "Problems in the theory and design of electromagnetic flowmeters for dielectric liquids. Part 3a. modelling of zero drift due to flux linkage between coil and electrode cables," *Flow Measurement and Instrumentation*, vol. 14, no. 3, pp. 65–78, 2003.

[12] A. I. Maalouf, "A validated model for the zero drift due to transformer signals in electromagnetic flowmeters operating with electrolytic conductors," *IEEE Sensors Journal*, vol. 6, no. 6, pp. 1502–1510, 2006.

[13] Xu, Ke-Jun, Wang, and Xiao-Fen, "Identification and application of the signal model for the electromagnetic flowmeter under sinusoidal excitation," *Measurement science and technology*, vol. 18, no. 7, p. 1973, 2007.